CURRENT TRANSFORMER USED AS A VOLTAGE SOURCE

D.V. Nicolae[1)], J.F.J. van Rensburg[2)] and M.J. Case[2)]
[1)] Tshwane University of Technology, Private Bag X017, 0116 Pretoria North, South Africa
[2)] Vaal University of Technology, Private Bag X021, Vanderbijlpark, 1900, South Africa
E-mail: danaurel@yebo.co.za, hannesvr@vut.ac.za, mikecase@global.co.za

Abstract. A direct alternating current source to voltage source converter, which does not employ energy storage components, is presented. Conversion is done by a current steering mechanism in the form of a current transformer with two secondary windings. The direct conversion concept, basic circuit, simulation and experimental results of a reduced scale model are presented.

Keywords: ac-to-ac converter, current-to-voltage converter, current transformer, transmission of electrical energy

1. INTRODUCTION

The power grid is a well-established system for the distribution of electrical energy, but the developing parts of Southern Africa tend to remain outside the scope of provision of a typical power system.
Non-conventional methods of extracting power from high voltage transmission lines are investigated worldwide in order to supply remote areas with small amounts of electric power [1], [2], [3].
The current transformer (CT) is one non-conventional method that is under investigation for quite some time [4]. Normally a current transformer is used for measurement and protection [5], [6]. In this study the CT is utilized as power device performing a direct conversion from alternating current to alternating voltage. Accordingly, the design of the CT assumes that operating at rated input current is normal. In the event of the current exceeding the rated value, it is assumed the protection system will come into operation.

2. DIRECT CONVERSION CONCEPT

The direct alternating current to alternating voltage conversion concept eliminates the need of the output inverter which reduces the power electronics component and thus increasing the reliability of the equipment.

2.1 Basic Circuit

Figure 1 shows the solution proposed for a CT to be used as power device that can achieve the direct conversion from alternating current to alternating voltage. The CT is equipped with two windings: main/load secondary and control winding.
The voltage controller picks up the output voltage, compare with the reference and via a microcontroller provides the control signal for the gate of the bilateral switch. The bilateral switch controls the current into control winding and thus the flux in the current transformer.

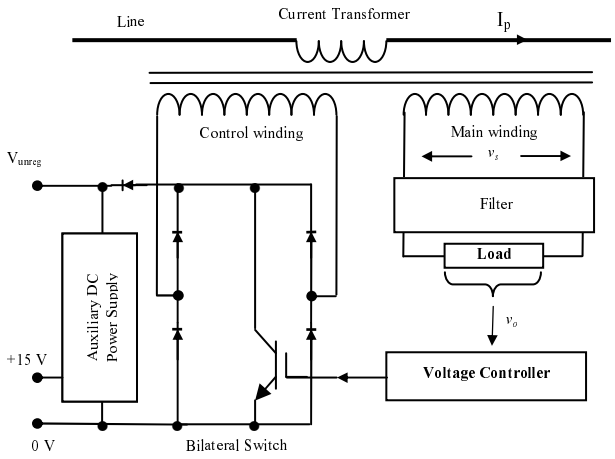

Fig.1. Basic circuit

One other function of the proposed circuit is recovering the energy passing through the control winding; when the bilateral switch is OFF, a pulse goes to the auxiliary DC power supply. The unregulated voltage will appear from the very beginning, thus eliminating the need of a back-up battery. Although the variation of the unregulated voltage is relatively high, it still can be used to power the associated electronics and some DC loads eventually.

2.2 Background

The load secondary (v_s) is designed for a voltage higher then the required output voltage. According to Faraday's law:

$$v'_s = -\frac{d}{dt}\Phi_p \tag{1}$$

But the primary flux Φ_p is directly dependant on the primary/main current i_p:

$$i_p(t) = I_p \sin \omega_p t \tag{2}$$

$$\Phi_p = C \cdot i_p \tag{3}$$

where C is a constant that depends on the geometry of the current transformer.

Thus:

$$v'_s = -C\omega I_p \cos\omega_p t \tag{4}$$

or

$$v'_s = V_s \sin\omega_p t \tag{5}$$

The control winding is designed such that when it is short-circuited the resulting current saturates the core irrespective of what happens in the load winding. At that moment: v_s = 0. When the switch is OFF, the secondary voltage is given by relation (5).

It should be pointed out that there are two frequencies in this system. One is the utility supply frequency (f_p = 50 Hz), and the other is the chopping/control frequency (f_c), which is much higher than the utility frequency. The situation described can be seen to be the same as that of a train of amplitude modulated pulses (Figure 2).

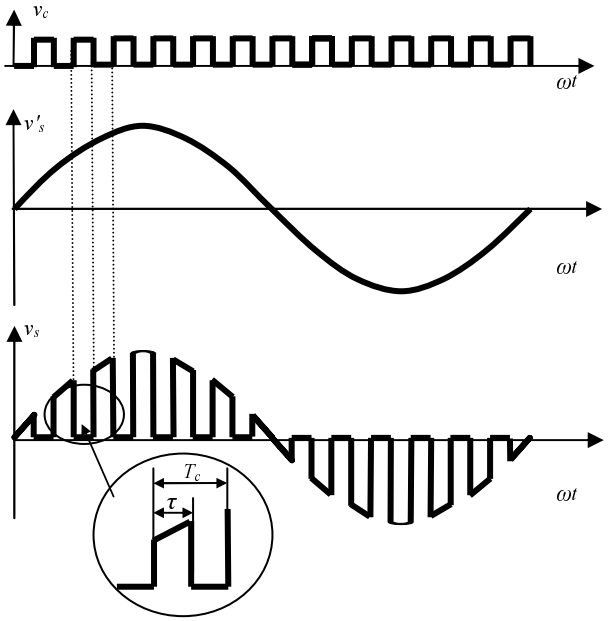

Fig.2. Secondary voltage generation

The mathematical expression for this waveform can be obtained as:

$$v_s(t) = v_c(t) \times v'_s(t) \tag{6}$$

where v'_s is given by (5) and v_c is the control signal with unit amplitude and that in Fourier series can be written as:

$$v_c(t) = \frac{\tau}{T_c} + \frac{2\tau}{T_c}\sum_{n=1}^{\infty} \frac{\sin\dfrac{n\omega_c\tau}{2}}{\dfrac{n\omega_c\tau}{2}} \times \cos n\omega_c t \tag{7}$$

Thus:

$$v_s(t) = (1-k)V_s \sin\omega_p t + V_s \sum_{n=1}^{\infty}\left\{\frac{\sin nk\pi}{\pi n}\left[\sin(\omega_p + n\omega_c)t + \sin(\omega_p - n\omega_c)t\right]\right\} \tag{8}$$

where k is the duty-cycle of the control signal on the gate of the switch. A more detailed derivation can be found in [7], [8] and [9]. By means of an LC low-pass filter the harmonic components will be adequately reduced and the output voltage will be:

$$v_o = (1-k)V_s \sin\omega_p t \tag{9}$$

Equations (4), (5) and (9) reveal that the load voltage v_o depends on the duty-cycle of the control frequency and the primary current. This shows that there is a direct conversion from an alternating current source to an alternating voltage source with the possibility of controlling the output voltage via the duty-cycle of the control winding.

3. SIMULATION RESULTS

Figure 3 shows the model used during the simulations; Matlab 6 was the simulation tool and the center block of the model was the saturated transformer (CT). During the simulation, the model was validated. One other task during the simulation was to find an optimum for the output filter and switching frequency.

A current source of 1500 A amplitude, the control voltage of 100V, the main/load voltage of 400V, a filter of L = 2 mH and C = 10 μF and a switch with R_{ON} = 1 Ω were considered.

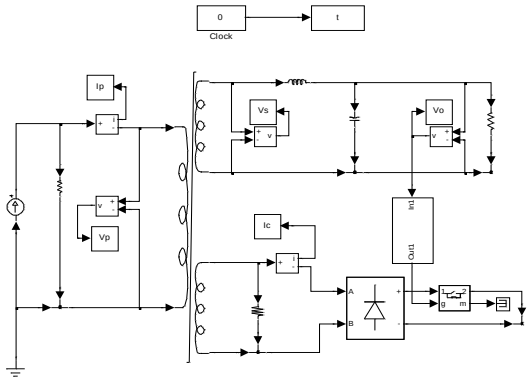

Fig.3. Simulation model

3.1 Basic function

Based on the above model, simulations to prove the main function have been performed; these include the dependency of the output voltage upon the duty cycle and influence of the switching frequency on output voltage.

Figure 4 shows the input current, secondary and output voltages for a switching frequency of 1 kHz with 80% duty-cycle. For a duty-cycle of 20%, the output voltage shows as in figure 5.

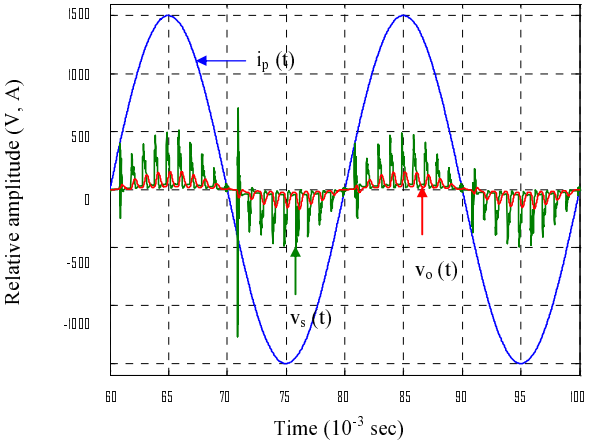

Fig.4. Output voltage for 1 kHz switching frequency and k = 80%

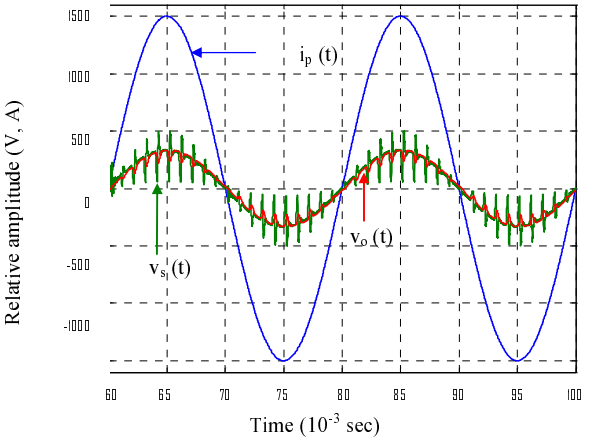

Fig.5. Output voltage for 1 kHz switching frequency and k = 20%

From figures 4 and 5 one can notice the influence of the duty-cycle and the ripple of the output voltage is relatively high. In order to decrease the output voltage ripple, the switching frequency was increase to 4 kHz; a much higher frequency could produce an almost perfect output voltage but the stress on the IGBT is also increased. Figure 7 shows the output voltage for switching frequency of 4 kHz with a duty-cycle of 50%.

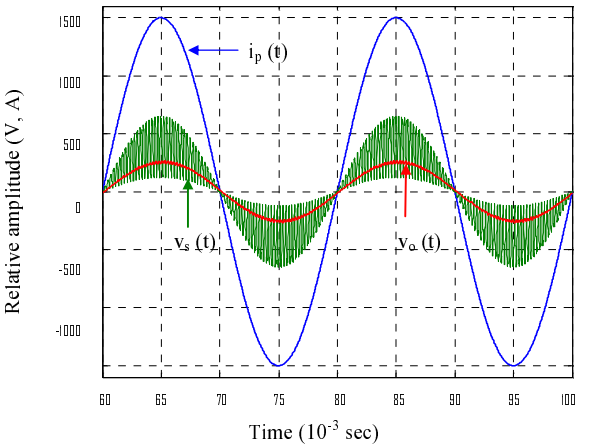

Fig.6. Output voltage for 4 kHz switching frequency and k = 50%

Another aspect investigated was the influence of this converter upon the transmission line. Figure 7 shows the input current and the voltage disturbance introduced by this device.

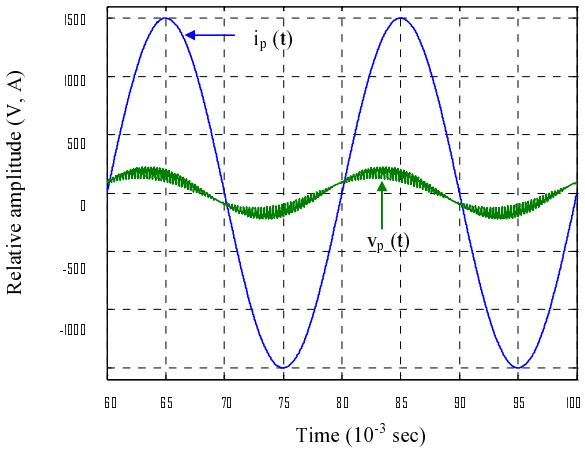

Fig.7. Input current & input voltage

As can be notice from figure 7, the influence on the transmission line is very small, practically negligible, while the load receives a power in the range of 3kW. The noise introduced by this method is small and is very much attenuated by the transmission line impedance.

3.2 Transient influence

Abnormal situations which include a step in load current, a normal step and a spike in input current .have been simulated. The simulation have been performed using a 4 kHz switching frequency which ensure a good quality of the output voltage while keeping a reasonable stress level into the switch.
Figure 8 shows the behavior of the model when the load current suddenly drops to half the value.

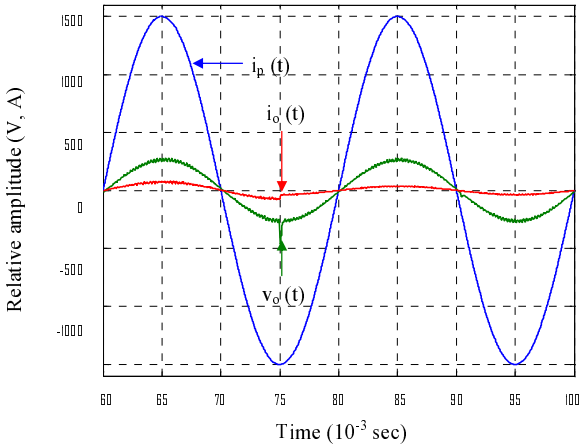

Fig.8. Impact of the step in output current

As can be noticed, when the current drops to half the voltage is unchanged.
Figure 9 shows the output voltage versus input current when the last one drops to forty percentage of its initial value. The

drop in the main line current is a gradually situation towards the end of the working but can also appear as sudden event.

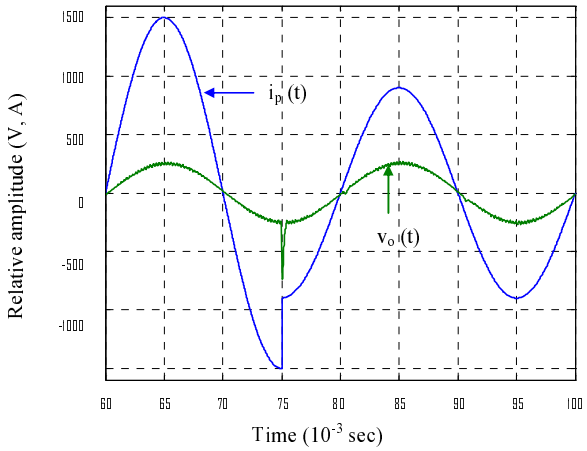

Fig. 9. Impact of input current step on output voltage

A situation more challenging such as a short spike in input current as high as ten times greater in amplitude and 10 milliseconds period is presented in Figure 10. This situation can happen quite often as results of lightning or pre-fault current in the transmission lines.

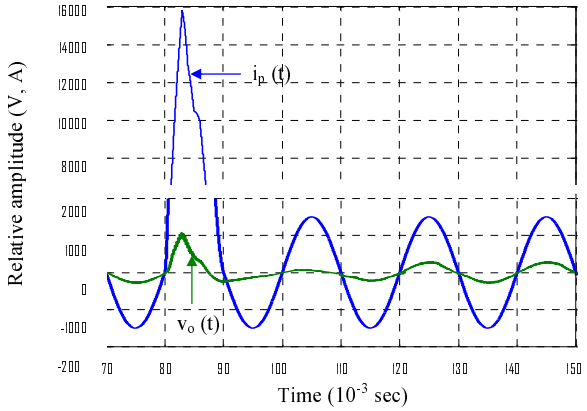

Fig. 10. Impact of a big input current transient

The influence produced by sudden spikes, as can be observed from the figure 10, consists of a dc component which appears and saturates the CT. This is converted into strong distortion of the wave form of the output voltage. Once the transient disappears, the dc component extinguishes itself and the wave form comes to normal. Because the main function of this application is not measuring, this effect is not critical.
The main concern regarding transients should be the inter-turn/layer capacitance that must be reduced as much as possible.

4. EXPERIMENTAL RESULTS

For validation, a small scale model has been built. An input current of 4.4 A_{rms} was generated and the output voltage was designed to maximum 60 V_{rms} for safety purposes; the load resistance was 430 Ω. For this model, as found during the simulations, a control frequency of 4 kHz has been used.
During experiments, the problem of synchronizing the switching frequency with the supply frequency has aroused. In order to keep a solution as simple as possible, there was no reference source for the supply frequency. The solution introduced was to allow a free oscillation for a very short period of time until the proper information (supply frequency) appeared after the low-pass filter. Then the duty-cycle control was activated.
Firstly, the duty-cycle was manually varied. The figures 11 and 12 show the output voltage measured for two different values of the duty-cycle.

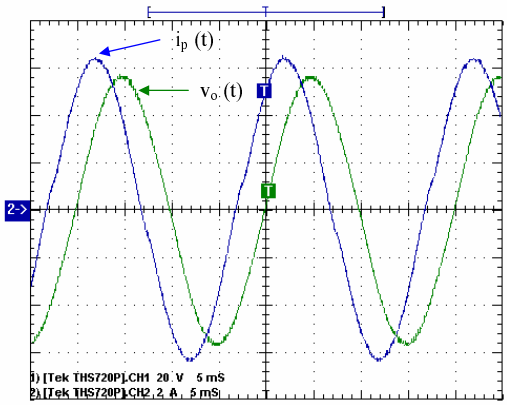

Fig. 11. Input current & output voltage for 30% duty cycle

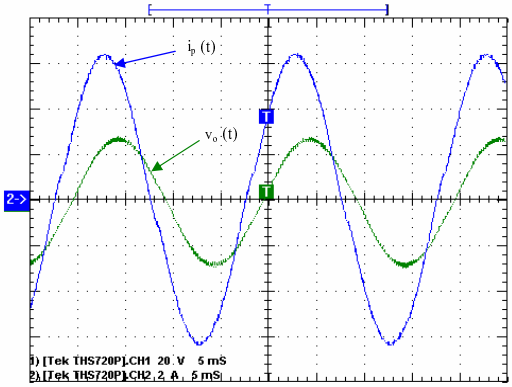

Fig. 12. Input current & output voltage for 70% duty cycle

The next step was to close the loop, set the output voltage to 40 V_{rms} and check the voltage regulation for a change in load from initial one of 430 Ω to double. Figure 13 shows the output voltage and the output current for the load of 430 Ω and figure 14 shows the same parameters for a load resistance of 860 Ω.

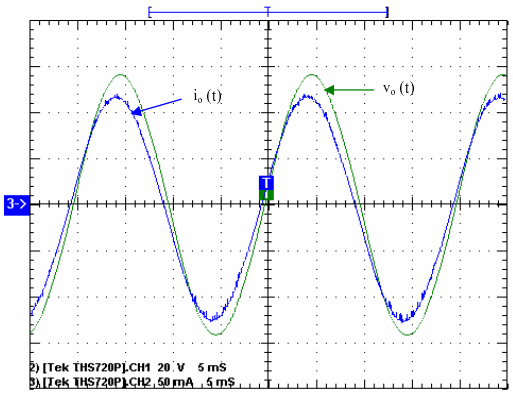

Fig. 13. Output current & output voltage for 430 Ω load

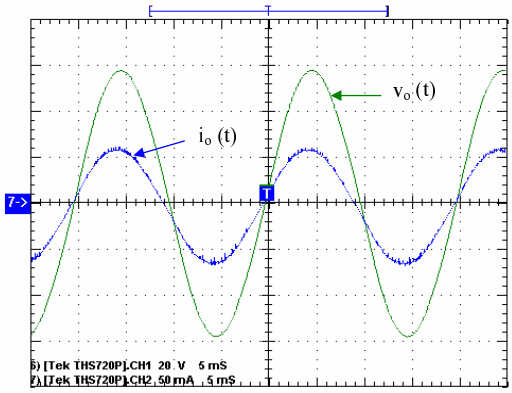

Fig. 14. Output current & output voltage for 860 Ω load

As can be notice from figures 13 and 14, the output voltage is constant when the current decreased to half.

5. CONCLUSIONS

Analyzing the experimental results, the conclusion drawn is that the concept of direct alternating current to alternating voltage conversion is valid.

The present study shows the feasibility of a CT-based direct alternating current source to voltage source converter, eliminating the need for the usual substation in remote areas where small amounts of electric power is needed. This method is simple and relatively easy to implement.

Simulation results show the functionality and behaviour under transient conditions of the proposed device. Although, the transient has an influence upon the model, still is not critical for the main function: delivering energy.

Based on these experimental results a more powerful model is under development [10]; the final goal is to reach a power of 5 to 10 kVA output.

This solution is indicated to be implemented on a three-phase system, for a substantial increase in output power. When a three-phase solution is implemented, the DC auxiliary power supply can be combined in one, resulting in a less variation of the unregulated voltage and a higher power capability on the DC side.

Using a sample and hold method combined with a digital processing algorithm, this device can also provide information about the current in the main line; when the bilateral switch is OFF, the pulse created depends on the duty cycle that is known (generated by the microcontroller) and the main current. In implementing this function, CT saturation algorithms such as [11] and [12] should be considered.

6. REFERENCES

[1] Bochard B, Bolduc L and Beaulieu G, "Capacitive divider substation". IEEE Transaction on Power Delivery, Vol. 12, No. 3, July 1997, pg. 1202-1209

[2] Berthiaume R and Blais R, "Microwave repeater power supply tapped from the overhead ground wire on 735 kV transmission line". IEEE Transaction on Power Apparatus and Systems, Vol. PAS-99, No. 1, pp. 183-184

[3] Nicolae DV, Janse van Rensburg JF and CASE MJ, "Rogowski Coil Power Application". 11th International Power Electronics and Motion Control Conference, 2-4 September 2004, Riga, Latvia, 2004.

[4] Janse van Rensburg JF & Case MJ, "Current transformer-fed power supply". EDPE 01 Conference. Podbanske: Slovakia, 2001.

[5] Jenkins DJ, "Introduction to Instrument-Transformers". George Newness Limited, London, 1967.

[6] Sachdev MS, Sidhu TS and Gill HS, "A Busbar Protection Technique and Its Performance During CT Saturation and CT Ratio-Mismatch". IEEE Transactions on Power Delivery, vol. 15, iss. 3, pp. 895-901, July 2000.

[7] Case MJ, "A Direct A.C. to A.C. Regenerative Frequency and Voltage Converter". PhD Thesis University of Cape Town, 1980.

[8] Conner FR, *Signals.* Edward Arnold (Publishers) Ltd. 1973.

[9] Addoweesh KE, "An exact analysis of an ideal static AC chopper". International Journal of Electronics, Vol. 75, No. 5, Taylor & Francis Ltd. 1993.

[10] Janse van Rensburg JF and Nicolae DV, "Current Transformer – based Direct Frequency Converter from Alternating Current Source to Alternating Voltage Source", Patent 01782005, January 10, 2005

[11] Kang Y.-C, Ok S.-H and Kang S.-H, "A CT Saturation Detection Algorithm". IEEE Transactions on Power Delivery, vol. 19, No. 1, pp. 78-85, January 2004.

[12] Fernandez C, "An Impedance-Based CT Saturation Detection Algorithm for Bus-Bar Differential Protection", IEEE Transactions on Power Delivery, vol. 16, No. 4, pp. 468-472, October 2001.